ASSESSMENT OF THE EFFECTS OF CLIMATE CHANGE ON SLOPE STABILITY USING LOCAL FACTOR OF SAFETY

Farsheed Bagheri, P.Eng.
GHD, Mississauga, Ontario, Canada
Ali Ghassemi, PhD, EIT and Rashid Bashir, PhD, P.Eng.
Department of Civil Engineering – York University, Toronto, Ontario, Canada

ABSTRACT
Climate change is expected to continue over this century with significant effect on climate variables such as precipitation. Consequent changes in water content within earth structures such as infrastructure embankments, can trigger local, shallow or global failures in currently stable slopes. The widely used limit equilibrium method (LEM) for slope stability assessment is not normally effective for capturing shallow failure modes. In this paper, the effect of climate change on the stability of embankments was quantified by estimating a field of Local Factor of Safety (LFS). For estimation of LFS, a coupled hydro-mechanical model equipped with soil-atmosphere boundary was applied. The effect of moisture content variation on the effective stress was taken into account using suction stress state. For the case study, the effects of climate change on the stability of a typical highway embankment in Ottawa, Ontario were quantified. The results indicate that not only larger mass of embankment will be influenced by local failures in next decades, but also the likelihood of substantial shallow failures increases. Contrary to LEM, the LFS method can trace future evolution of potential shallow failures.

RÉSUMÉ
Les changements climatiques devraient se poursuivre au cours de ce siècle avec des effets importants sur les variables climatiques telles que les précipitations. Les modifications consécutives de la teneur en eau dans les structures terrestres, telles que les remblais d'infrastructure, peuvent provoquer des défaillances locales, superficielles ou globales sur des pentes actuellement stables. La méthode d'équilibre limite (LEM) largement utilisée pour l'évaluation de la stabilité des pentes n'est normalement pas efficace pour capturer les modes de défaillance peu profonds. Dans cet article, l'effet du changement climatique sur la stabilité des digues a été quantifié en estimant un champ de facteur de sécurité local (FSL). Pour l'estimation de l'EPA, un modèle couplé hydro-mécanique doté d'une limite sol-atmosphère a été appliqué. L'effet de la variation de la teneur en humidité sur la contrainte effective a été pris en compte en utilisant l'état de contrainte d'aspiration. Pour l'étude de cas, les effets du changement climatique sur la stabilité d'une digue d'une autoroute typique à Ottawa, en Ontario, ont été quantifiés. Les résultats obtenus indiquent que non seulement une masse plus importante de remblais sera influencée par les défaillances locales au cours des prochaines décennies, mais également que la probabilité de défaillances importantes à faible profondeur augmente. Contrairement à LEM, le domaine de FLS peut retracer l'évolution des défaillances potentielles peu profondes dans le futur.

1 INTRODUCTION

Climate change is a long-term shift in weather conditions primarily identified by changes in temperature. Changes to the climate system is unequivocal and Canada is one of the countries that is warming at a fast rate (IPCC 2013). Climate warming will result in changes of other important climate variables, such as precipitation, and potential evaporation. Climate change involves both changes in average conditions and changes in variability, including frequency and intensity of extreme weather events.

Soil embankments and slopes are important class of geotechnical infrastructure in transit and transportation networks. Due to permanent exposure to the environment, stability of embankments is highly dependent on climate variables. Precipitation and evaporation are the two important climate variables that control the water balance at the embankment surface. The pore pressure distribution in the embankment is dependent on the water balance at the embankment surface. Increase in pore water pressure can reduce the shear strength of the unsaturated soil materials and can adversely affect the stability of embankments. The slope instability may develop within the embankment, or through the base as local, surficial (shallow), general, or deep-seated failure. As schematic of various failure types is shown in Figure 1 (Han et al., 2004).

Numerical simulation of climate change impact on slope stability requires a multi-disciplinary approach. It includes a climate model to provide high-resolution future climate dataset as well as a hydrological model to simulate variably saturated flow due to soil-atmosphere interaction. Further, a proper geotechnical model is required for slope stability assessment considering the effects of suction on shear strength of the soil. Several researchers have proposed numerical models for investigation of climate change impacts on the stability of slopes (e.g. Collison et al. 2000; Rouainia et al. 2009; Robinson et al. 2017; Pk et al. 2018). Even though the soil-atmosphere interaction (precipitation and evaporation) are more likely to cause shallow and local failures, most of the previous studies have only considered the general or deep-seated failures using the conventional limit equilibrium methods.

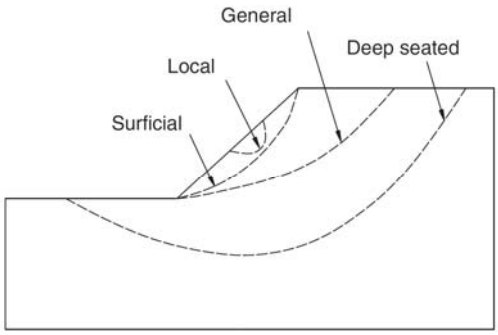

Figure 1. Potential Slope Stability Failures (modified from Han et al. 2004)

Embankments are normally designed to satisfy a minimum factor of safety (FOS) against global failures that would impact the operation of the roadway. Potential surficial and local failures are generally considered to be repaired as part of operation and maintenance (O&M). However, the substantial impact of climate change on water balance of the earth embankments may results in a significant O&M issues over the infrastructure lifetime. In addition, while the local slope failure and erosion are two different technical subjects, often are not distinguished properly in design and O&M investigation processes. Observations show that in contrast to erosion that may erratically occur on different areas of a slope surface, local slope failures are more likely to spread from toe of the slope (Figure 2). It is also worth mentioning that uncontrolled shallow failures may finally lead to global slope failures in the future.

Figure 2. Example of local failure (Ontario 400 Series)

This study is a part of an ongoing research on the effects of climate change on the stability of highway embankments across Ontario. The objective of current study is to investigate the effect of climate change on the stability of earth fill embankments against shallow and local failures by estimating the field of Local Factor of Safety (LFS). In order to accomplish this objective, a coupled hydro-mechanical model equipped with soil-atmosphere boundary condition using unsaturated flow formulation was developed. The effect of water content variation on in situ effective stress field is applied using the suction stress state concept within the unsaturated soil mechanics framework. For the current study, the effect of long-term climate change on surficial stability of a typical highway embankment in the Ottawa area was investigated. Historical climate data (i.e. 1981-2010) and future climate data (i.e. 2010-2100) for the city of Ottawa was used in the study.

2 STUDY OF LOCAL FAILURES USING LFS FIELD

The most widely used analytical technique to carry out slope stability analyses is limit equilibrium (LE) method of slices. Stress-strain behavior is not considered in LE method and a factor of safety is calculated basically by comparing shear strength versus shear stress in small slices of slope. The LE method is known to be an effective and reliable method of slope stability analysis.

Although, theoretically there is no limitation on depth of failure in LEM, it is a common practice to specify a minimum sliding mass depth in limit equilibrium analyses to not consider shallow slip surfaces. This minumum slip depth is usually defined around 1.0 to 1.5 m. As mentioned before, failures shallower than such assumptions are generally considered too shallow that would affect operation and maintanace procedures. In addition, LEM typically seeks a single stability indicator for the entire slope. Thus, even considering lower value for minimum sliding mass depth, LEM cannot provide local failure zones that might be the location of initial future global failures (Lu et al., 2012).

In this study, the stability of slopes against shallow and local failures was numerically investigated by calculating a scalar field of local factor of safety (LFS). These kinds of failures have more potential to be triggered due to climate change impact than global or deep-seated failures. Furthermore, these mechanisms are not normally assessed in traditional slope stability analyses using LEM.

Local factor of safety (LFS) is the ratio of Coulomb stress of the potential failure state under the Mohr-Coulomb criterion (τ^*) to the Coulomb stress at the current state of stress (τ) (Lu et al., 2012):

$$LFS = \frac{\tau^*}{\tau} \qquad [1]$$

Figure 3 illustrates the definition of τ^* and τ for a given Mohr circle stress state on a shear stress-normal stress space. As can be seen on this figure, while the state of stress in a slope represented by the Mohr circle is below the Mohr-Coulomb failure envelope, the LFS is greater than unity. LFS can also be easily derived based on the mean and deviator effective stresses (p' and q') in two-dimensional space as follows (Lu et al., 2012):

$$LFS = \frac{2\,cos\emptyset'}{q'}\,(c' + p'\tan\emptyset') \qquad [2]$$

where c′ is the drained cohesion of the slope material, ϕ′ is the drained friction angle of the slope material. LFS

can be calculated at each point using Equation 2. LFS contour map that can be obtained by joining the points with same LFS values indicating an accurate stability condition for a given slope. The zones with LFS greater than unity imply statically stable conditions. While, zones with LFS equal or less than unity, are at the limit state and local failure can be expected.

It should be noted that soil-atmosphere interaction (precipitation and evaporation) affects the PWP distribution through embankment fill over time. This leads to the evolution of the effective stress fields that consequently affects the LFS field. The changes in effective stress field can be estimated by calculating the suction stress based on single stress state variable framework (Lu and Likos, 2006). A brief review of the framework is as follows.

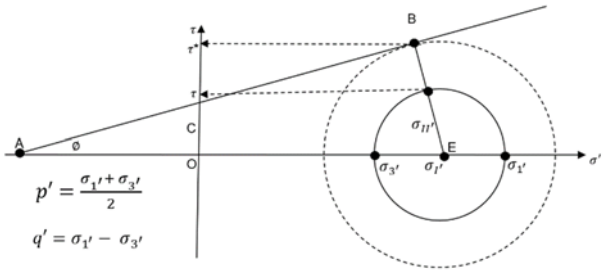

Figure 3. Illustration of definition of τ* and τ for a given Mohr circle stress state (Adopted from Lu et al., 2012)

3 SINGLE STRESS STATE VARIABLE FRAMEWORK

Matric suction or negative pore pressure has the effect of increasing the shear strength of unsaturated soils. Therefore, considering the contribution of matric suction in the slope stability assessment is of great importance (Fredlund et al. 2012; Adem and Vanapalli 2015; Arairo et al. 2015). Two common frameworks to take into account the effect of matric suction on shear strength are two independent stress state variables (e.g. Coleman 1962; Bishop & Blight 1963; Fredlund and Morgenstern 1977; Fredlund et al. 1996, Vanapalli et al. 1996) and single stress state variable framework (e.g. Bishop 1954; Bishop 1959; Lambe 1960; Lu and Likos 2006). In first approach, unsaturated shear strength is a function of the two stress variables: net normal stress and matric suction. The most frequently used method based on two stress state variables is as follows (Vanapalli et al. 1996):

$$\tau = c' + (\sigma - u_a)\tan\phi' + (u_a - u_w)[(Sr)\tan\phi'] \quad [3]$$

where c` is effective cohesion, $u_a$ is pore-air pressure, $u_w$ is pore-water pressure, $\sigma - u_a$ is net normal stress on the failure plane, $u_a - u_w$ is matric suction, $\phi$` is effective angle of internal friction for the saturated soil and Sr is the degree of effective saturation as described below:

$$Sr = \frac{\theta - \theta r}{\theta s - \theta r} \quad [4]$$

where θ is the volumetric water content, and θ_s and θ_r are saturated and residual volumetric water content, respectively.

Despite its popularity, two stress state variable approach is subjected to a major practical limitation: It cannot be utilized within the context of classical mechanics that consider effective stress as the single stress state variable governing the soil behavior (Lu et al. 2010). To overcome this limitation, Lu and Likos (2006) extended the pioneering work by Bishop (1954 and 1959), to define a new stress variable called suction stress (σ_s) within the context of Terzaghi's effective stress equation as following:

$$\sigma' = (\sigma - u_a) - \sigma^s \quad [5]$$

Lu et al. (2010) proposed a closed-form expression for suction stress for the full range of matric suction:

$$\sigma^s = -(u_a - u_w) \qquad u_a - u_w \le 0 \quad [6]$$

$$\sigma^s = \frac{(u_a - u_w)}{(1 + [\alpha (u_a - u_w)]^n)^{(n-1)/n}} \qquad u_a - u_w \ge 0 \quad [7]$$

where α and n are the parameters used to define the soil water characteristic curve (SWCC) of a soil using van Genuchten's (1980) equation. Suction stress can also be expressed as a function of effective stress as following (Lu et al., 2010):

$$\sigma^s = -\frac{S_e}{\alpha}\left(S_e^{\frac{n}{1-n}} - 1\right)^{\frac{1}{n}} \qquad 0 \le S_e \le 1 \quad [8]$$

In this study, the single stress state approach by Lu et al. (2006, 2010) was used to develop hydro-mechanical models that capture the evolution of effective stress field in variably saturated embankments subjected to soil-atmosphere interaction. The effective stress field is the basis for developing LFS contours as explained in section 2. In addition, two stress state variable model by Vanapalli et al. (1996) was employed to estimate the shear strength of unsaturated soil through limit equilibrium analyses.

4 NUMERICAL MODEL

4.1 Geometry and Material

The embankment profile considered in current study represents a typical highway embankment in the province of Ontario, Canada. Since the problem is symmetrical, only one-half of the domain as shown in Figure 4, was simulated. The height of embankment was considered to be 8 m. This is the maximum allowable height of earth fill embankment without berms in Ontario (OPSD 202.010). Side slopes of embankment are 2 horizontal to 1 vertical (2H:1V) with a 3 m width unpaved shoulder at the top of embankment. The distance between the slope toe and the

right side of the model was set to three times the height of the slope to minimize the influence of the side boundary condition (Rahardjo et al., 2010). The water table was conservatively assumed at the natural ground surface that is 4 m below the level of slope toe.

In this paper, a sandy material typically used in the construction of highway embankments in Ontario was selected for numerical simulations. The mathematical model suggested by van Genuchten (1980) was used to represent the soil water characteristic curve (SWCC) as shown in Figure 5a. The unsaturated hydraulic conductivity function (HCF) for the sandy material was determined from SWCC using the van Genuchten Mualem approach (Mualem 1976, van Genuchten 1980). Figure 5b shows the suction stress characteristic curves (SSCC) that was estimated using Equation 8. The soil parameters for the sandy material used in development of these curves are those reported by Bashir et al. (2018).

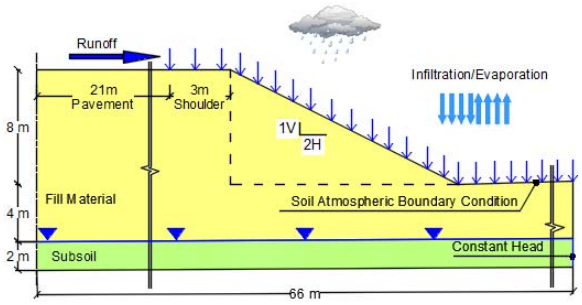

Figure 4. Design profile of the highway embankment

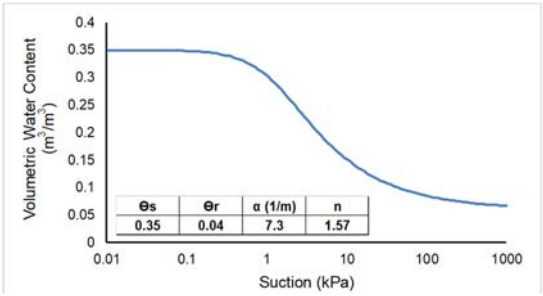

(a)

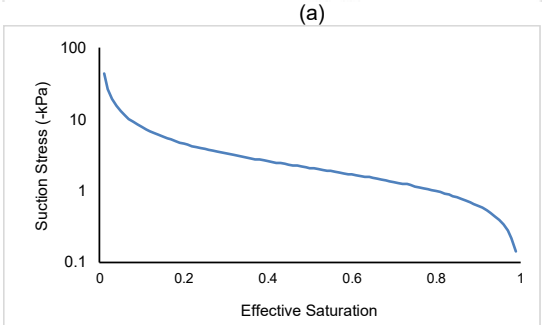

(b)

Figure 5. Hydraulic soil properties: (a) SWCC; (b) SSCC

All embankment fill materials to be used in MTO projects are to be placed and compacted in accordance with the provincial standards, OPSS 206 and OPSS 501. An effective friction angle of 32° is usually assumed for fill materials placed and compacted in accordance with above mentioned standards. For in-situ stress analysis, the value of Poisson's ratio that controls the development of horizontal stresses was assumed 0.3 for the sandy material.

4.2 Design Climates

In this study, two sets of design climates were used to investigate the effect of climate change on slope stability of the embankment.

The first set of design climates was selected to study the effects of changes in daily climate variables over long period of time (i.e. 120 years). There are several available sources for future climate data based on different General Circulation Models (GCM) and Representative Concentration Pathways (RCP). General Circulation Models such as Had GEM2 or GFDL-ESM2M are the most commonly used climate models based primarily on physical laws that describe the atmospheric and oceanic dynamics and physics (IPCC 1996). Representative Concentration Pathways refer to different climate futures. Each pathway is considered possible depending on how much greenhouse gases are emitted in the years to come. There are four different RCPs namely RCP 2.6, 4.5, 6.0 and 8.5. The RCPs are named after a possible range of radiative forcing values in the year 2100. For example, RCP 2.6 refers to a radiative forcing value of 2.6 W/m^2. Therefore, Representative Concentration Pathway with highest radiative forcing value (RCP 8.5) represents the worst case scenario. In this study, future climate data (i.e. 2011-2100) from GCM Had GEM2 and RCP 8.5 as well as 30 years of historical climate data (i.e. 1980-2010) for Ottawa were used as the first set of design climates

The second design climate dataset comprised of the intensity-duration-frequency (IDF) curves, to investigate the effect of occurrence of extreme precipitation in the region on the stability of the embankments. Future IDF curves for the city of Ottawa were sourced from Ontario Climate Change Data Portal (CCDP 2017). A detailed review indicated that a significant increase in future extreme precipitation during the last 30 years period of this century (i.e. 2070-2100) can be expected. In this research, IDF curves by CCDP based on RCP8.5 were taken as the critical scenario for this period. A range of durations (1, 6, and 24 hours) based on 100 years return period were considered for development of design storms.

4.3 Hydro-Mechanical Model

In this study, HYDRUS 2D (Šimůnek et al. 2006) was used for analyzing the variation of water balance distribution through the embankment subjected to historical and future climate datasets. HYDRUS 2D is a finite element software that numerically solves the Richards' equation for analysis of water flow in variably saturated soil. The software utilizes a system-dependent boundary condition that controls the maximum amount of water that can either evaporate or enter the boundary.

In seepage analyses, the pavement at the top of the embankment was modeled as a no flow boundary. A no

flow boundary was also assigned to the left side and bottom of the domain. At the right hand boundary, the groundwater table was applied to be 4 m below the level of slope toe using a constant head boundary (Figure 4). The runoff from the pavement was assumed to be distributed over the earth fill embankment.

To compute the field of in situ stresses, Slope Cube module (Lu et al. 2016) of the HYDRUS 2D software package was used. This supplemental module computes the soil stresses and displacements by using the field of moist unit weight as the gravity term by using a two-dimensional finite element code for plane stress linear elasticity analysis. In situ total stress analysis was carried out with the left and right boundaries free to move in the vertical direction; while the bottom boundary is fixed in both vertical and horizontal directions (Figure 4). The LFS field is eventually estimated by the CUBE module using the PWP distribution form HYDRUS 2D for calculation of suction and effective stresses.

4.2 Limit Equilibrium Analyses

The results of LFS model were compared with stability assessments using LEM. The widely used limit equilibrium software SLOPE/W together with seepage software SEEP/W was used. Both these software are modules of a software suite called GeoStudio (Geo-Slope International Ltd. 2016) and can be coupled very easily. The coupling ensures the continuous calculation of FOS of slopes by SLOPE/W for each time step, for which pore pressure distribution is available from the seepage analysis by SEEP/W. Morgenstern-Price method (Morgenstern and Price 1965) that considers both the static force and moment equilibrium was applied in limit equilibrium analyses. The strength due to suction in unsaturated soil was estimated using Equation 3.

In limit equilinbrium analyses, two different values of minumum slip mass depth were considered. A minimum slip depth of 1.0 m was examined in the first group of LE analyses to capture the FOS against general failure. In the second group, minimum slip mass depth of 0.3 m was assumed. This was to consider the shallower failures in LE analyses that are more comparable with LFS results.

5 RESULTS AND DISSCUSSION

5.1 LFS Field vs. Global Factor of Safety

As part of this study, the developed hydro-mechanical model was applied to assess the stability of the embankment subjected to Ottawa historical climate data (i.e. 1981-2010). The climate dataset comprised of daily records of precipitation and potential evaporation. Evaluations as part of this study as well as previous studies (Pk. et al. 2018) have indicated that lower factors of safety have a positive correlation with the embankment saturation. Intuitively this makes sense as higher saturation would imply lower suction contribution to strength and larger contribution of PWP to instability. Therefore, time history of embankment saturation was evaluated to identify the time at which the embankment has the highest saturation. Stability assessment were carried out at this critical time. In addition to LFS analysis by CUBE module of the HYDRUS 2D, LE analysis was also carried out by SEEP/W and SLOPE/W assuming a minimum slip depth of 1.0 m for slip surface.

Figure 6 compares the obtained results using these two different methods. As can be seen in this figure, LE method suggests a FOS value of 1.42 for the critical slip surface. Using Cube module, LFS contour of 1.42 has been drawn in this figure. LEM critical slip and LFS contour of 1.42 are relatively similar; however, LFS contour is more irregular than LEM output, which follows an ideal circular pattern. While LEM method indicates deeper slip surface within the slope crest, LFS contours show more critical situation at the toe of slope. The LFS profile for the value of 1.0 is also depicted in Figure 6. The result indicates that a shallow area of the slope could potentially fail under the considered climatic conditions.

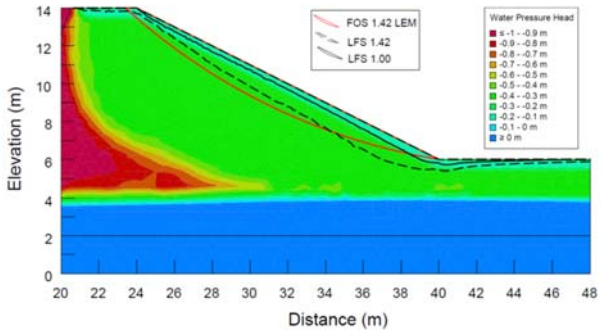

Figure 6. LEM critical slip surface and LFS contours

5.2 Long-Term Variation of LFS

Assessment of the evolution of LFS field in the slope mass due to the effects of changes in daily climate variables over long period of time is presented in this section. The defined first set of design climate data for Ottawa including 30 years of historical climate data (i.e. 1980-2010) and 90 years of predicted future climate data (i.e. 2011-2100) was applied as soil-atmosphere boundary in the developed hydro-mechanical model.

In limit equilibrium analyses, a single factor of safety (FOS) represents the condition of the entire domain. However, in LFS method, a local factor of safety (LFS) is calculated for every point in the domain. Thus, a map of LFS contours that trace lines of equal LFS values can be established. Although LFS contour maps can present a general display of slope stability conditions, a quantitative LFS indicator is required particularly when the variation of LFS over time is of interest. Area of LFS<w footprint, measured in the numerical model cross section, was identified as $A_{LFS<w}$. For example, the value of $A_{LFS<1}$ is the area of zone in which LFS is less than unity. Obviously, this value represents the mass of local failure zone in a two-dimensional model.

A FORTRAN code was developed to calculate the $A_{LFS<w}$. Table 1 presents the minimum, maximum and average values of $A_{LFS<1}$ obtained from numerical simulation for 120 years daily climate data. It is noteworthy

that the minimum $A_{LFS<1}$ value is greater than zero. It indicates that there is always a potential for local failures over the time. The average value of 4.6 m^2 which is approximately 7% of slope area (the area encompassed by dashed line in Figure 4) is subjected to local failure. In addition, as presented in Table 1, more than half of the local failure zone area would be occurring in the downslope area (between toe and middle of slope). Simply it means the area adjacent to the toe of slope is more vulnerable.

According to the obtained results, the maximum of $A_{LFS<1}$ during historical period (i.e. 1980-2010) is 7.7 m^2 (12 % of slope area). In Figure 7, the maximum $A_{LFS<1}$ considering next 90 years data with an interval of 30 years are compared. It shows that the maximum predicted area of the local failure zone increases slightly. Moreover, the number of events that $A_{LFS<1}$ exceeds its maximum value during historical period is depicted on Figure 7. As can be seen, the above noted occurrences will demonstrate increasing trend in future.

Table 1. LFS<1.0 Area percentage within the slope area

	Minimum	Maximum	Average
$A_{LFS<1}$ (m^2) [%]	2.3 [1.5]	8.4 [13.2]	4.6 [7.2]
Downslope Area(%)	62	100	75

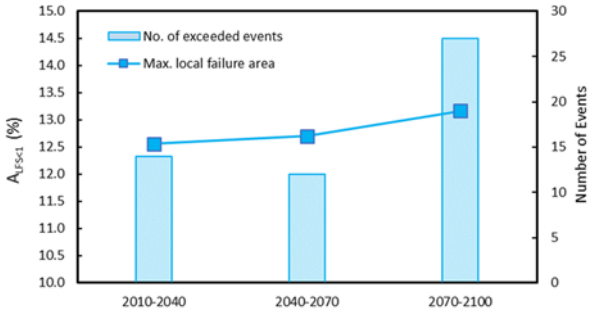

Figure 7. Long term evolution of LFS field

5.3 Evaluation of Local Slope Instabilities due to Future Extreme Events

Ideally, actual storms should be used in a hydrologic analysis. However, actual storm records are not usually available for every location particularly when the effects of future climate are under study. Therefore, establishment of synthetic storm hyetographs was considered in this study. There are several methods for generating design storm hyetographs in the literature. In some methods, a simple function is defined for intensity distribution of storm over time for a single point of the IDF curves. The simplest form is rectangular hyetographs, where a uniform intensity is used throughout the storm duration (Prodanovic and Simonovic 2004). Alternatively, geometric forms such as triangular hyetographs (e.g. Yen and Chow 1980) or linear/exponential hyetographs (e.g. Watt et al. 1986) have also been proposed. As an alternative of using a single point on an IDF curve, methods have been proposed that use the entire set of duration-intensity values for a particular return period and duration (e.g. Keifer and Chu 1957). The method proposed by Keifer and Chu (1957), known as the Chicago design storm, has been widely incorporated in Canadian practice (Marsalek and Watt 1984). The method also has been suggested by MTO to be applied for assessment of the storm impacts to the drainage systems (MTO 1997). In this study, the Chicago method was applied for providing intensity distribution over time for future extreme precipitation events. Figure 8 shows the 100 year storm event developed based on future IDF curve for different rainfall durations. The initial PWP distribution for these set of numerical analyses was based on the time in which the embankment has the highest saturation during historical period (i.e. 1980-2010)

Figure 9 presents the variation of $A_{LFS<1}$ over time for 1-hr, 6-hr and 24-hr storm durations. During 1 hour precipitation, area of local failure zone increases until the end of the storm. The rate of increase is higher within the peak time of storm hyetograph. In contrast to 1-hr rainfall, for 6-hr and 24-hr rainfall, $A_{LFS<1}$ increases up to a maximum value that is approximately corresponds to storm hyetograph peak. After the peak, it decreases until completion of the event as the water introduced during the initial part of storm dissipates within this time frame. From the design perspective, maximum value of $A_{LFS<1}$ should be addressed in slope stability calculations. Comparison of all three storm durations confirms that the 24-hr rainfall would have more adverse impact on the extent of local failure zone; however, the difference is not substantial.

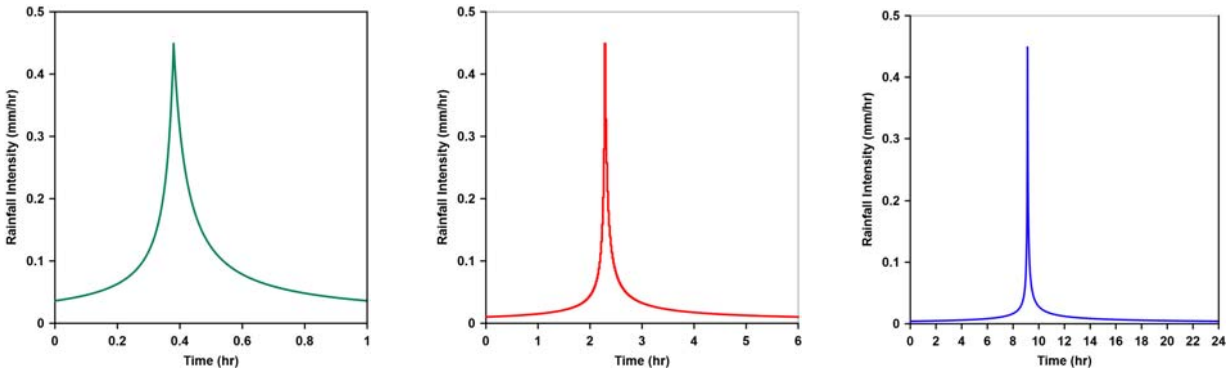

Figure 8. Chicago design storm for different storm durations

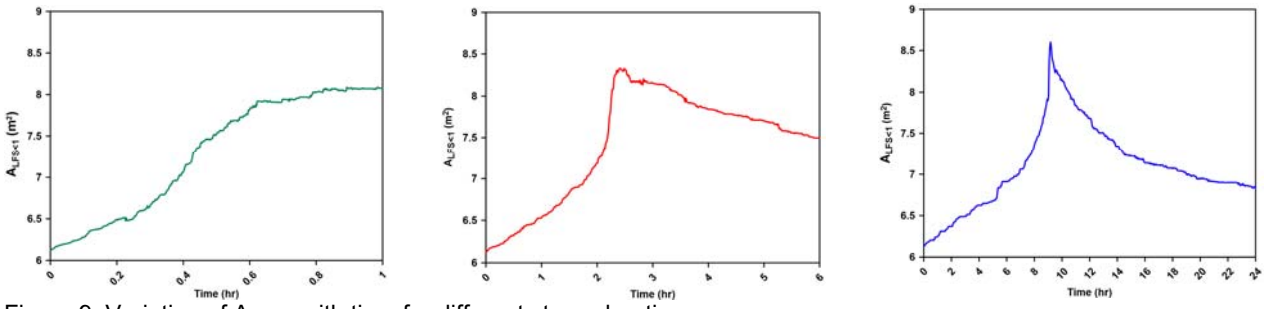

Figure 9. Variation of $A_{LFS<1}$ with time for different storm durations

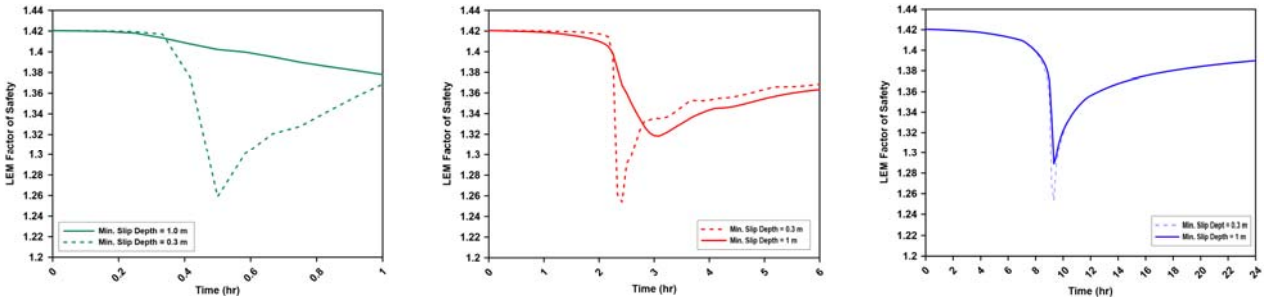

Figure 10. Variation of FOS with time for different storm durations

To compare the results of LFS-based analysis with traditional LE method, the same problem was simulated using coupled SEEP/W-SLOPE/W numerical model as described in Section 4.3. The results of the analyses conducted considering two minimum slip mass depths are shown in Figure 10. The minimum factor of safety is equal to 1.38, 1.32 and 1.29 for 1-hr, 6hr and 24-hr storm durations, respectively (with no slip depth less than 1.0 m). All obtained FOS value are greater than the commonly acceptable FOS of 1.3 for highway embankment design. Moreover, a minimum slip mass depth of 0.3 m was assumed in second set of LE analyses to consider the shallow failures that is more in line with LFS results. As shown in Figure 10, a lower minimum FOS was obtained for all three storm durations corresponding to the peak time of design storm hyetograph. It implies that extreme events have more intensive effects on potential shallower failures. It is also noteworthy that the obtained minimum FOS values for all three cases varying between 1.25 to 1.26. No values less than unity indicates that adjusting the minimum slip depth may not necessarily lead to identificationof shallower failure using conventional LE methods.

6 CONCLUDING REMARKS

In this study, the impact of climate change on stability of a typical highway embankment in the Ottawa area was investigated considering potential local failures. Earth embankments are more prone to shallow rather than general or deep-seated failures due to change in climate variables. However, such mechanisms are not normally assessed in traditional slope stability analyses using LEM. The applied approach in this study includes calculating a scalar field of local factor of safety (LFS) based on the field of effective stresses from stress-strain finite element analysis. To capture the variation of soil water content subjected to climate variables, a 2D transient variably saturated flow finite element model equipped with soil-atmosphere boundary was used. The results of hydrological model are introduced into the mechanical model using suction stress which has been recently proposed as a stress state variable to take into account the effect of matric suction on normal effective stresses.

Overall, the results of the study show that the developed numerical model is capable of investigating the adverse effects of climate change on shallow instability of embankment slopes. Not only larger mass of slope is predicted to be influenced by local failures in next decades, but also the likelihood of substantial shallow failures increases. At least for the current case, the area of local failure zone is changing over the time with more than half within the downslope zone. Furthermore, numerical simulation of slope stability subjected to future storms was conducted using both LEM and LFS methods. The results imply that contrary to LFS results that demonstrates high potential of shallow failure, LEM may not be able to identify this type of failure even by adjusting the minimum mass slip depth.

7 REFRENCES

Adem, H. and Vanapalli, S. 2014. Soil–environment Interactions Modelling for Expansive Soils, *Environmental Geotechnics*, 3(3): 178-187.

Arairo W., Prunier F., Djeran-Maigre I. and Millard A. 2015. Three Dimensional Analysis of Hydraulic Effect on Unsaturated Slope Stability, *Environmental Geotechnics* 3(1): 36–46.

Bishop, A. W. and Blight, G. E., 1963. Some Aspects of Effective Stress in Saturated and Unsaturated Soils. *Geotechnique*, 13: 177-197.

Bishop, A.W. 1959. The Principle of Effective Stress. *Teknisk Ukeblad*, 39: 859–863.

Bishop, C. 1954. Coden versus Sigils. *Journal of the American Society for Information Science*, 5(1): 28.

CCDP. 2017. Ontario Climate Change Data Portal. Available from http://www.ontarioccdp.ca.

Coleman, J. D. 1962. Stress-strain Relations for Partly Saturated Soil. *Geotechnique*, 12(4): 348-350.

Collison, A., Wade, S., Griffiths, J. and Dehn, M. 2000. Modelling The Impact of Predicted Climate Change on Landslide Frequency and Magnitude in SE England. *Engineering Geology*, 55(3): 205–218.

Fredlund, D. G. and Morgenstern, N. R. 1977. Stress State Variables for Unsaturated Soils. *Journal of Geotechnical and Geoenvironmental Engineering, American Society of Civil Engineering*, 103(5): 447–466.

Fredlund, D.G., Rahardjo, H. and Fredlund, M.D. 2012. Unsaturated Soil Mechanics in Engineering Practice. Wiley, Hoboken, NJ, USA.

Fredlund, D.G., Xing, A., Fredlund, M.D. and Barbour, S.L. 1996. The Relationship of The Unsaturated Soil Shear to The Soil-Water Characteristic Curve. *Canadian Geotechnical Journal*, 33(3): 440–448.

Geo-Slope International Ltd. 2016. Stability Modeling With SLOPE/W: An Engineering Methodology (Computer Program). *GEOSLOPE/W International Ltd*. Calgary, Alberta, Canada.

Han, J., Sheth, A.R., Porbaha, A. and Shen, S.L. 2004. Numerical Analysis of Embankment Stability Over Deep Mixed Foundations. ASCE Geotechnical Special Publication No. 126: 1385–1394, Geotechnical Engineering for Transportation Projects, GeoTrans 2004, ASCE. Los Angles, California, USA, July 26–31.

IPCC. 2013. Summary of IPCC, 2013. Summary for Policymakers. Climate Change 2013. The Physical Science Basis. Contribution of Working Group I to the Fifth Assessment Report of the Intergovernmental Panel on Climate Change [Stocker, T.F., D. Qin, G.-K. Plattner, M. Tignor, S.K. Allen, J. Boschung, A. Nauels, Y. Xia, V. Bex and P.M. Midgley (eds.)]. Cambridge University Press, Cambridge, United Kingdom and New York, NY, USA.

Keifer, C.J. and Chu, H.H. 1957. Synthetic Storm Pattern for Drainage Design. *Journal of the Hydraulics Division*, 83(4): 1–25.

Kramer, S.L. 1996. Geotechnical Earthquake Engineering. Prentice Hall, Upper Saddle River, N.J.

Lu, N., and Likos, W.J. 2006. Suction Stress Characteristic Curve for Unsaturated Soil. *Journal of Geotechnical and Geoenvironmental Engineering*, 132(2): 131–142.

Lu, N., Şener-Kaya, B., Wayllace, A. and Godt, J.W. 2012. Analysis of Rainfall-Induced Slope Instability Using a Field of Local Factor of Safety. Water Resources Research, 48(9).

Lu, N., Wayllace, A., Formetta, G., 2016. The Slope Cube Module. Soil Water Retention, LLC: Madison, WI, USA.

Marsalek, J. and Watt, W.E. 1984. Design storms for urban drainage design. *Canadian Journal of Civil Engineering*, 11(3): 574–584.

Morgenstern, N.R. and Price, V.E. 1965. The Analysis of The Stability of General Slip Surface. *Geotechnique* 15(1): 79-93.

MTO 1997. Drainage Management Manual, Ronin House Publishing, under contract from Ministry of Transportation of Ontario, Ottawa, Ontario, Canada.

Mualem, Y. 1976. A New Model for Predicting The Hydraulic Conductivity of Unsaturated Porous Media. Water Resources Research, 12(3): 513–522.

OPS 2014. OPSS.PROV 206: Construction Specification for Grading. OPS, ON, Canada.

OPS 2016. OPSD. 202.010. Slope Flattening Using Surplus Excavated Material On Earth or Rock Embankments.

OPS. Ontario Provincial Standards for Roads and Public Works 2010. OPSS 501. Construction Specification for Compacting. OPS, Ontario, Canada.

Pk, S., Bashir, R., and Beddoe, R. 2018. Effect of Climate Change on Earthen Embankments in Southern Ontario, Canada. *Environmental Geotechnics*: 1–70.

Prodanovic, P., and Simonovic, S. 2004. Generation of Synthetic Design Storms for the Upper Thames River Basin. Water Resources Research Report, Available from https://ir.lib.uwo.ca/wrrr/15.

Rahardjo, H., Nio, A.S., Leong, E.C., and Song, N.Y. 2010. Effects of Groundwater Table Position and Soil Properties on Stability of Slope during Rainfall. Journal of Geotechnical and Geoenvironmental Engineering, 136(11): 1555–1564.

Robinson, J.D., Vahedifard, F., and AghaKouchak, A. 2017. Rainfall-triggered slope instabilities under a changing climate: comparative study using historical and projected precipitation extremes. Canadian Geotechnical Journal, 54(1): 117–127.

Rouainia, M., Davies, O., O'Brien, T., and Glendinning, S. 2009. Numerical modelling of climate effects on slope stability. Proceedings of the Institution of Civil Engineers - Engineering Sustainability, 162(2): 81–89.

Šimŭnek, J., Van Genuchten, M.T., and Šejna, M. 2006. The HYDRUS software package for simulating two-and Three-Dimensional Movement of Water, Heat, and Multiple Solutes in Variably Saturated Media. Technical manual, version 1: 241.

van Genuchten, M.Th. 1980. A Closed Form Equation for Predicting the Hydraulic Conductivity of Unsaturated Soils. 44: 892–898.

Vanapalli, S.K., Fredlund, D.G., Pufahl, D.E. and Clifton, A.W. 1996. Model For The Prediction of Shear Strength With Respect To Soil Suction. *Canadian Geotechnical Journal*, 33(3): 379–392.

Watt, W.E., Chow, K.C.A., Hogg, W.D., and Lathem, K.W. 1986. A 1-h Urban Design Storm For Canada. *Canadian Journal of Civil Engineering*, 13(3): 293–300.

Yen, B.C., and Chow, V.T. 1980. Design Hyetographs for Small Drainage Structures. *Journal of the Hydraulics Division*, 106(HY6).